Measuring the Solar zone of avoidance for the MeerKAT antennas

Document number	M2600-0000-049
Revision	
Classification	
Prepared By	T. Mangena
Approval Date	June 2023

Organisation	:	NRF (National Research Foundation)
Facility	:	SARAO (South African Radio Astronomy Observatory)
Project	:	MeerKAT
Document Type	:	Report
Function/Discipline	:	Science commissioning

DOCUMENT APPROVALS

	Name	Designation	Affiliation	Date	Signature
Released By	T. Mangena	Data analyst	SARAO		T.MANGENA T.MANGENA (Jun 8, 2023 09:42 GMT+2)
Reviewed By	M. Gouws	Systems analyst	SARAO		Marcel Gouws Marcel Gouws (Jun 8, 2023 15:44 GMT+2)
Reviewed By	S. Passmoor	Senior Operations Scientist	SARAO		Passmoor
Approved By	S. Goedhart	Manager: Science operations and commissioning	SARAO		S.Goedhart Sharmila Goedhart (Jun 9, 2023 11:19 GMT+2)

DOCUMENT HISTORY

Revision	Date Of Issue	Prepared By	Comments (e.g. ECN Number or changes to document)

DOCUMENT DISTRIBUTION

DOCUMENT SOFTWARE

Package		Version	Filename
Word Processor	Google drive		SSA-0001E-001 Rev 03 SSA General Document Template_03.04.2019

COMPANY DETAILS

Name	SARAO, Cape Town (Observatory, Cape Town)	SARAO, HartRAO (Hartebeeshoek, Gauteng)	SARAO, Karoo Astronomy Reserve (Carnarvon, Northern Cape)
Physical / Postal Address	2 Fir Street, (North Entrance Black River Park, Observatory, Cape Town, 7925	P.O.Box 443, Krugersdorp, 1740, South Africa	Posbus 69, Carnarvon, 8925, South Africa
Tel.	+27 21 506 7300	+27 12 301 3100	+27 21 506 7300
Fax.	+27 21 506 7375	+27 12 301 3300	+27 86 538 6836
Website	www.ska.ac.za	www.hartrao.ac.za	www.ska.ac.za

TABLE OF CONTENTS

Abstract

We measure the solar zone of avoidance for the three receivers (L-band, UHF-band, S-band) of the MeerKAT radio telescope by comparing the system temperature (T_{sys}) as a function of the solar angular separation ($\boldsymbol{\theta}_{sun}$). The solar contribution of the antenna's system temperature is evident when moving away from the Sun. The angular separation at which we observe a zero solar contribution to the T_{sys} is $\boldsymbol{\theta}_{sun}$~ 4.5 (L-band), 6.9 (UHF-band), 5.2 (S0-band), 3.9 (S4-band) degrees measured from the centre of the Sun respectively. But within this separation the system temperature is strongly affected by the Solar radiation. When pointing away from the Sun (i.e when angular separation is greater than obtained $\boldsymbol{\theta}_{sun}$ for each band), the antenna system temperatures ranging from 18K - 22K for L-band, 16K - 21K for UHF-band, 16K - 27K for both S0-band and S4-band are observed. The UHF-band is much more sensitive to solar radiation due to its large beam size, followed by L-band, S0 and lastly S4. We note that investigating zone of avoidance based on imaging capabilities will give us more accurate constraints of $\boldsymbol{\theta}_{sun}$.

Introduction

The effect of solar radiation into the radio telescope observation can be severe when observing the source close to the Sun. In this work we determine how close to the Sun in terms of angular separation can MeerKAT radio telescope observe a source without suffering the consequence of severe data contamination. We do so by analysing the change of antenna system temperature (T_{sys}) when performing a scan across the Sun. There are several contributions to the system temperature of a radio antenna,which can be separated into several different contributions as follows:

$$T_{sys} = T_{bg} + T_{sky} + T_{spill} + T_{loss} + T_{cal} + T_{rx} \qquad (1)$$

where T_{bg} is noise contribution from microwave and galactic background, T_{sky} is noise contribution from atmospheric emission which can be approximated using the eq. $T_{sky} = T_{sky}(1 - e^{-\tau o csc\ E})$ where $\boldsymbol{\tau}_o$ = zenith opacity, E = elevation angle. T_{spill} is noise contribution from ground radiation (spillover and scattering), T_{loss} is noise contribution due to losses in feed, T_{cal} is noise contribution due to injected noise and T_{rx} is the receiver noise temperature. Note that T_{bg}, T_{sky} , and T_{spill} vary with position on the sky, therefore, their sum can be regarded as the antenna temperature (T_a),

$$T_a = T_{bg} + T_{sky} + T_{spill} \qquad (2)$$

There are calibration procedure to be applied to radio data in order to account for all these different contributors. The nominal antenna system temperature of MeerKAT antennas is within the range 16K - 27K. Bright sources increase the system temperature when its power enters the receiver chain. This is due to the relationship between the flux of the sources and antenna temperature shown by the following equation :

$$S = 2kT_a v^2/c^2 \Delta v \qquad (3)$$

where S is the source flux, T_a is the antenna temperature. According to equation (1) and (2), the antenna temperature is then related to the T_{sys} . This shows how the antenna temperature is proportional to the beam power pattern with the brightness temperature distribution of the source. We aim to establish an understanding of the behaviour of the antennas when observing very close to the sun based on the system temperature, and use this information to determine a zone of avoidance for MeerKAT observations running during the day. In the next section we will look into the procedure followed in this work, mainly the observational setups, section 3 focuses on analysis of our work, we present the results in section 4 and conclude in section 5.

PROCEDURE

We observe the Sun using the available MeerKAT antennas with 3 different receivers and 4 different bands. The following table summarises the information on each observation.

Table 1 : Summary of used observational parameter for MeerKAT telescope in this work.

Receiver/Band	Frequency range (MHz)	Correlator product	# of antennas
L	900 - 1670	c856M1k	63
U	580 - 1015	c544M1k	61
S0 (2187.5)	1750 - 2625	c875M1k	58
S4 (3062.5)	2625 - 3500	c875M1k	58

From Table 1 above, each band has its frequency range as indicated on the second column. We include two different bands for the S-band receiver; these are the S0 and S4 bands. For this investigation we use a scan pattern which performs one scan across the Sun with constant elevation. The scan duration and scan extent differs per band. This is due to the beam width of a band ($\theta \simeq \lambda/D$). For L-band and S-band observation we set scan-duration = 300s and scan-extent=25 and for U-band observation scan-duration = 600s and scan-extent=50 which is double that of L-band parameters. The elevation is kept constant and scan through a range of azimuth across the source. To calibrate the observation we turn on the noise diode, which injects a known temperature into the receiver chain before and after the observation. The observations for each band were conducted on different days. However, we can neglect the solar activity effect as all observations were conducted within the same month. The different number of antennas in Table 1 is due to availability of antennas on that particular day. The next section covers how we performed data calibration and analysis on the acquired dataset to investigate the solar zone of avoidance.

Analysis

We perform our data calibration and analysis using the single-dish continuum analysis package (SCAPE), which is built on the katdal framework. The data is a three dimensional visibility array (e.g. time, frequency, correlation product) and is stored using a Redis database (.rdb). We use the SCAPE to access the observation metadata which includes the correlator configuration, antenna details, receiver and noise diode serial numbers models. We use the SCAPE functions to convert the raw autocorrelation measurements in the dataset to calibrated temperatures. The SCAPE package locates the change in levels caused by switching the noise-diodes on and off and uses the appropriate noise diode models, determined via serial number, to convert the polarisations to temperatures.

The dataset contains 3 scans. Figure 1 shows the time series plot for L-band with a side power spectrum plot for two polarizations (HH and VV). Referencing on the upper plot, the first scan shown by the red arrow reading from left to right is for when the antenna's noise diode is turned on(for 60 seconds) before the source is observed. This scan is flagged out as it happens during antennas's slewing to the target. The second scan shown by the second arrow represents target (Sun) scan showing much stronger change in frequency and the third arrow indicates the third scan for when the antennas noise diode is turned on for 60 seconds after the source is observed. The parts where the frequency showing less to no variation is when the telescope is pointing away from the source.

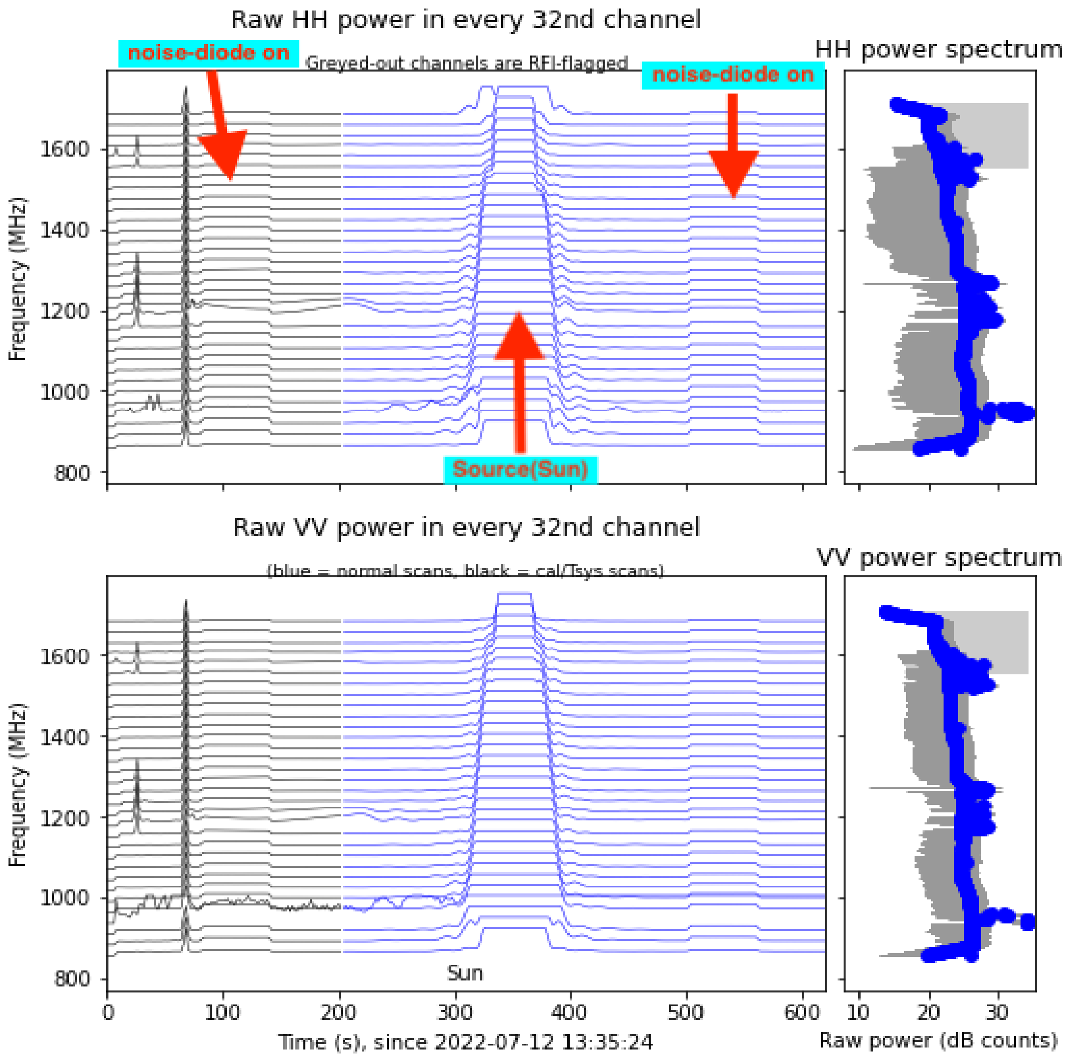

Figure 1 : *The time series plot for L-band showing 3 observational scans indicated by a red arrow on the first upper HH polarisation figure, with on side frequency plot included. The bottom figure shows similar plots for VV polarisation.*

After calibrating the data into temperature values, we remove the noise diode data and just use the scan across the Sun. We calculate the angular separation by taking the square root of the sum of the target coordinates squared for the selected scan. This returns 1d separation angular points for the source scan. The corresponding temperature data comes from taking a mean of selected polarisation scan data using **dataset.scan[i].pol(X).mean** where i is the scan number index and X is the chosen polarisation. The calibration procedure is done for all antennas used in the observations and the temperature results are regarded as T_{sys} for each antenna. Note that for all bands analysis, we exclude m060 due to its bad noise-diode. This leaves us with 62 antennas in L-band for the calculations. We further exclude m024 due to the unavailable noise diode model in UHF-band analysis, this leaves us to 59 antennas eligible for analysis in UHF-band. The S-band analysis was done using data from 47 antennas for S0 and 53 for S4 respectively. Five antennas in both bands were removed from the analysis due to not having the noise diode model files available and the remaining were excluded due to poor noise diode performance.

We furthermore create bins by grouping data points of each antenna by their entries. This means that the data points in each antenna occupying entry 0 (index) forms the first bin. Since we have

179 data points in each antenna, we end up with 179 bins with 62 data points in L-band, 59 in UHF-band, 47 in S0-band and 53 in S4-band. We calculate the mean for each bin and use the results as a representation of the system temperature of each band. The interpolation technique is then used to determine the value of angular separation where the system temperature is tolerable. We achieve this by calculating the mean system temperature of the first 50% of the data and use it to calculate its corresponding angular separation using an interpolation function. We have observed that the data for each band behaves significantly differently, therefore, we test four different interpolation functions (cubic, nearest, next, quadratic) and consider the best results based on empirical results. Cubic method fits a different cubic polynomial between each pair of data points. Nearest method inserts the value of the interpolated point to the value of the most adjucent point working the same as "next" method. Quadratic method uses second order spline interpolation. We find good results using "nearest" on L-band, "next" on UHF-band, "cubic" on S0 and "quadratic" on S4.

The interpolation function for each band is generated by passing the mean temperature and mean solar angle into 1d interpolation method. The function is then used to determine the solar angle at which the solar contribution to system temperature is negligible. We do so by calculating the mean system temperature of the first 50% of data points and find the corresponding solar angle at 3 sigma level using the interpolation function generated. The Table 2 and figure 6 on the next section summarises the results for each band.

Results

We present the results for four bands(L-band, UHF-band, S0-band, S4-band) of the MeerKAT telescope where we show a plot of T_{sys} of selected antennas used in the observation against angular separation for each band and for all bands combined to make a comparison. Figure 2 shows the results for L-band (H polarisation) where we can see a decline in temperature when moving away from the source(Sun). The mean fit represented by a black line shows a clear exponential decline together with antenna data points represented by the faded cyan dots.
The following table summarises the results for all four bands.

Table 2 : Summary of the calculated angular separation for each band.

Band	Solar angular separation where solar radiation causes tsys to increase[degrees]	Solar angular separation[degrees] (for the targets & calibrators)
L-band	4.50	10
UHF-band	6.90	15
S0-band	5.20	9
S4-band	3.87	6

We see that from $\boldsymbol{\theta}_{sun}$~ 4.5 degrees the system temperature reaches a stable trend starting from T_{sys} = 21.32 K(median) with a very minimal deviation, this is supported by the small error bars from that separation going to higher values of θ_{sun}. This indicates that from that angular separation there is no longer solar contribution into the system temperature. We observe the same trend in V polarisation and omitted the results for V polarisation in all bands (The slight increase in system temperature at around θ_{sun}= 8.5 in L-band might be from a background source, as it is not present on the other side of the scan across the Sun.)

Figure 3 shows the results for UHF-band, note that the UHF-band has double scan-extent of L-band, hence the angular separation is also double that of L-band.
From this figure we can see a similar trend of temperature declining when moving away from the source. The system temperature reaches stable state from θ_{sun}= 6.9 with T_{sys} = median(17.90 K). We furthermore show the results for S-band in figure 4 (S0-band) and figure 5(S4-band) respectively. Both S0 and S4 show an early steep decline reaching a stable state at θ_{sun}= 5.2 degrees(S0) and θ_{sun}= 3.8 degrees(S4).

We then compare the results of all bands in Figure 6 where we show the averaged plots for all four bands plotted together. The figure shows a plot of T_{sys} against angular separation θ_{sun} where we can observe a clear but slight distinction in system temperature trend between the four bands. The dotted lines with the same colour as per plots represent the obtained angular separation for each band. All system temperatures before the dotted lines for each band are regarded as containing the solar contribution.

Given the presented results, we advise that the solar angular separations for all targets in science observations conducted during the day are summarized in table 2, in column 2. Column 3 is for all calibrators in each bands. We note that considering conducting our investigation of the solar zone of avoidance using imaging capabilities will improve our results. We leave the imaging part for future work.

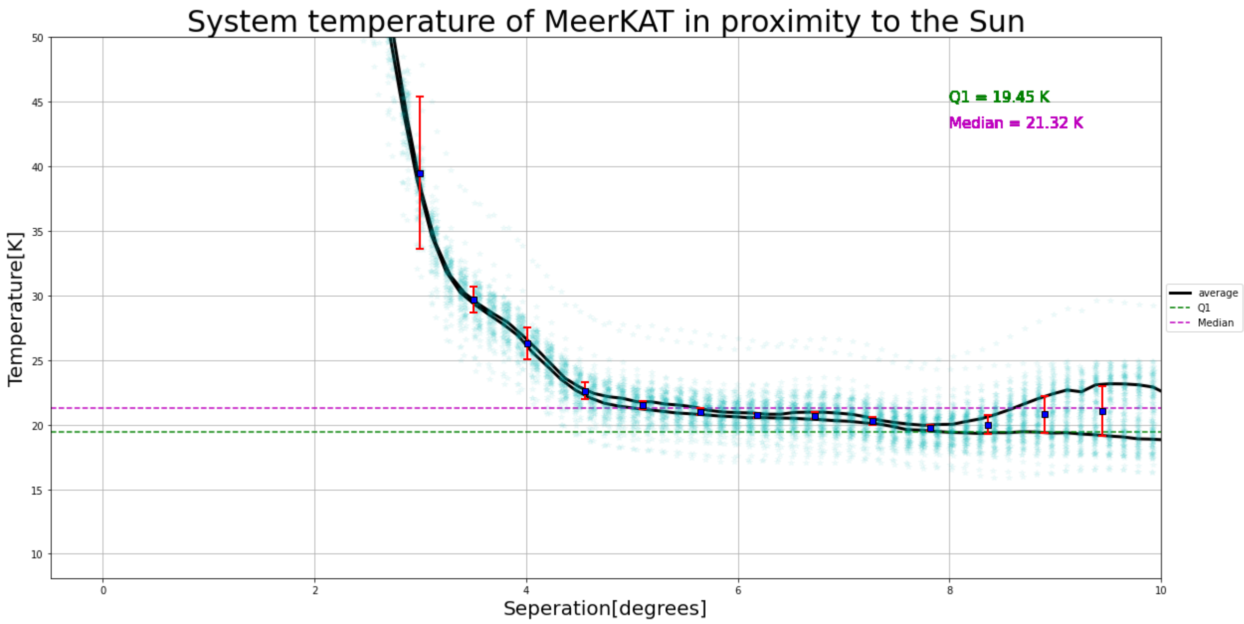

Figure 2 : *The plot of system temperature vs angular separation for L-band with error bars. The cyan faded points show the data from all antennas used in the analysis and black solid lines represent the mean fit calculated from antennas data points. The pink and green lines represent the median and lower quartile.*

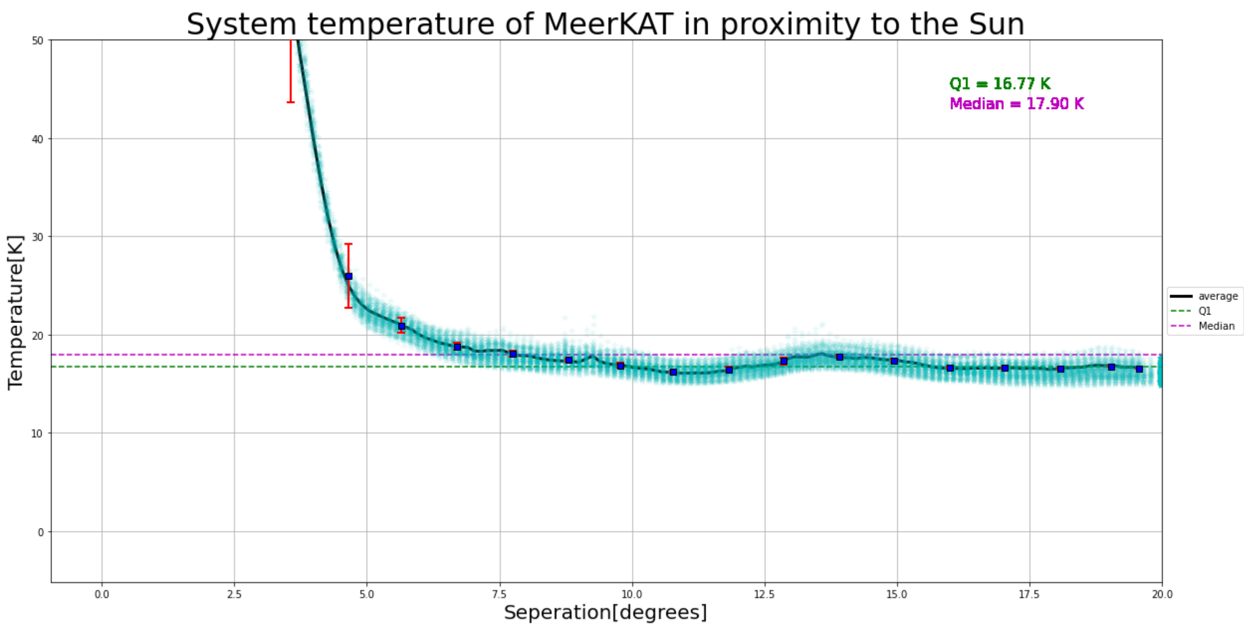

Figure 3 : *The plot of system temperature vs angular separation for UHF-band with error bars. The cyan faded points show the data from all antennas used in the analysis and black solid lines represent the mean fit calculated from antennas data points. The pink and green lines represent the median and lower quartile.*

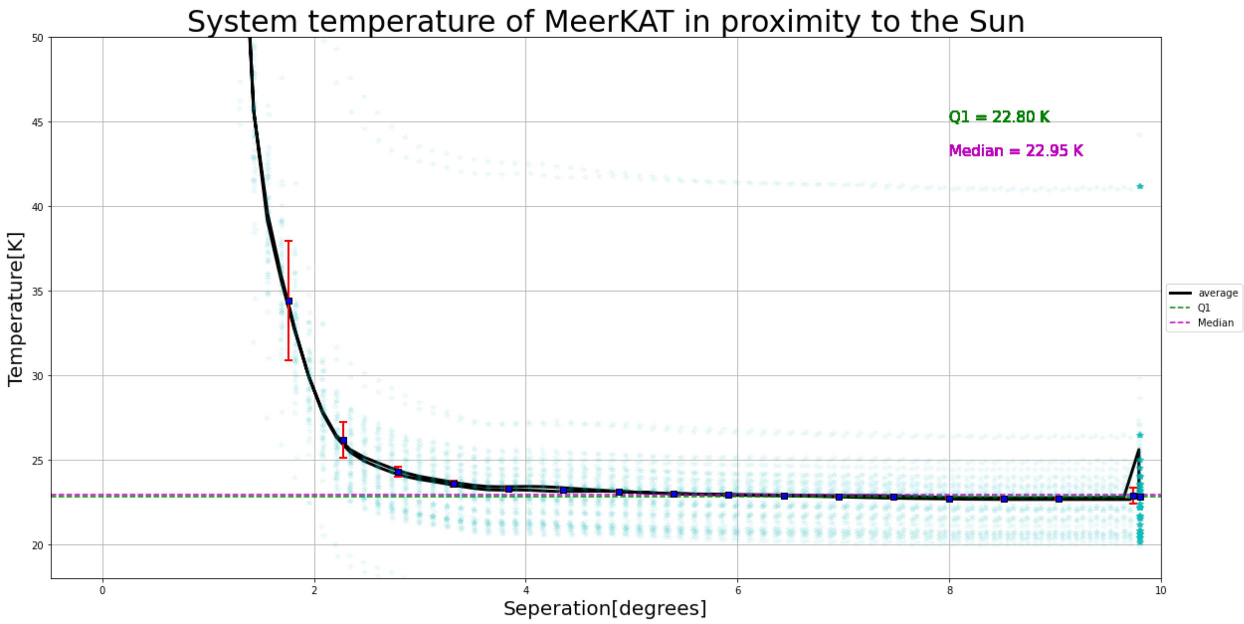

Figure 4 : *The plot of system temperature vs angular separation for S0-band with error bars. The cyan faded points show the data from all antennas used in the analysis and black solid lines represent the mean fit calculated from antennas data points. The pink and green lines represent the median and lower quartile.*

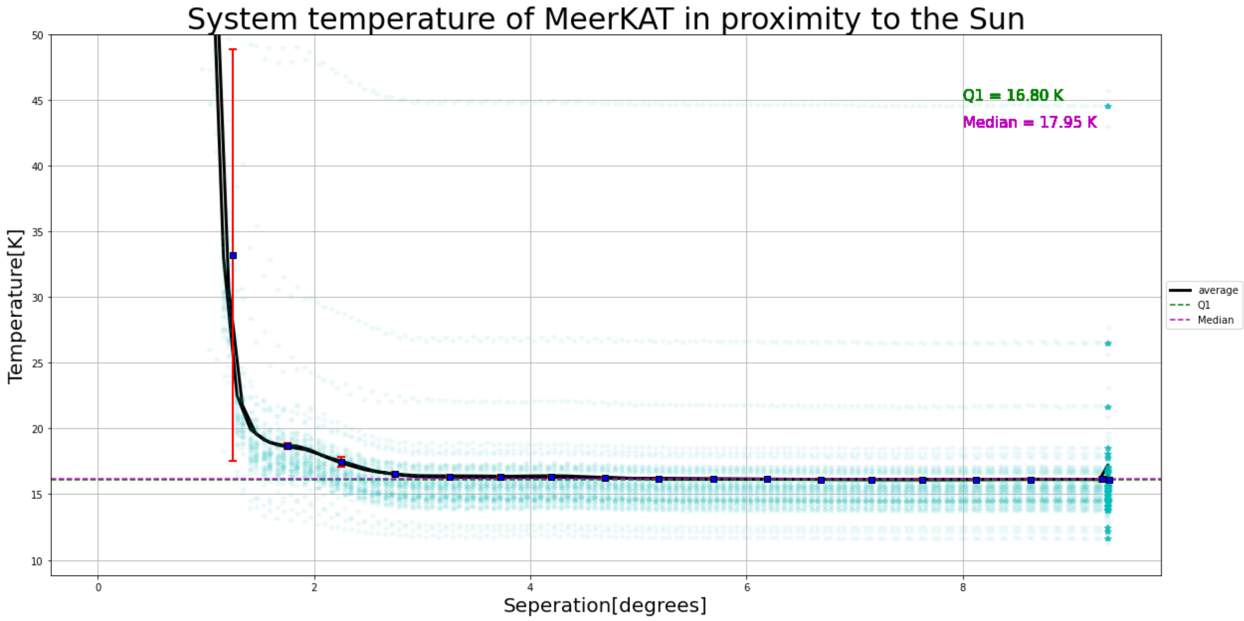

Figure 5 : *The plot of system temperature vs angular separation for S4-band with error bars. The cyan faded points show the data from all antennas used in the analysis and black solid lines represent the mean fit calculated from antennas data points. The pink and green lines represent the median and lower quartile.*

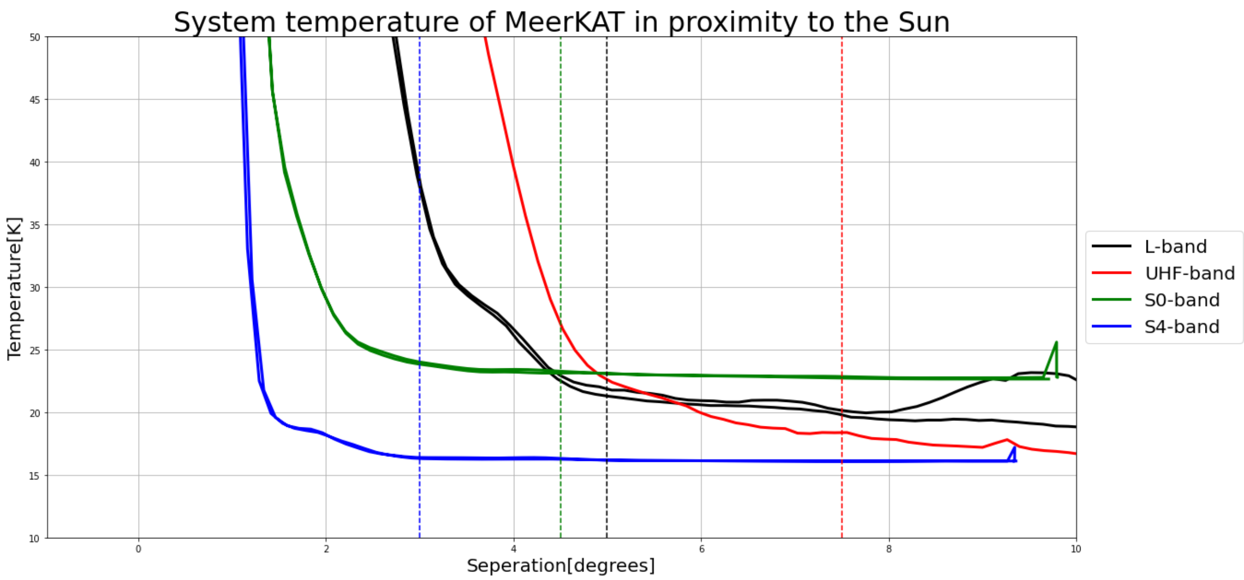

Figure 6: *The plot of system temperature vs solar angular separation for all four bands. The blue line represents the averaged S4-band with its angular separation cut shown by the blue vertical line, the green line shows the averaged S0-band with its corresponding angular separation cut shown by a green vertical line. The black line shows the averaged L-band plot with vertical black line as its angular separation cut and the red plot shows the averaged U-band and its angular separation cut is represented by the red vertical line.*

Conclusion

We investigated the solar zone of avoidance for the L-band, UHF-band and the S-bands of the MeerKAT radio telescope. The analysis shows that the solar contribution to the system temperature is minimal for solar angular separations of θ_{sun}~ 4.5 (L-band), 6.9 (UHF-band), 5.2 (S0-band), 3.9 (S4-band) which are summarised in Table 2. The UHF-band is severely affected by solar contribution, followed by L-band, S0 and lastly S4. The results indicate that we can observe 4.5 degrees close to the Sun without the risk of contamination from solar contribution in L-band, 6.9 degrees in UHF-band, 5.2 degrees in S0-band, and 3.9 degrees in S4-band. We further advise that a more stringent zone can be achieved by looking at imaging capabilities.

Solar avoidance radius

Final Audit Report 2023-06-09

Created:	2023-06-08
By:	Carmen Humphreys (carmen@ska.ac.za)
Status:	Signed
Transaction ID:	CBJCHBCAABAAS-wMnpSpm6yoUcHmyn0R78bqpdRkO4P7

"Solar avoidance radius" History

Document created by Carmen Humphreys (carmen@ska.ac.za)
2023-06-08 - 7:35:22 AM GMT- IP address: 209.203.45.25

Document emailed to tmangena@sarao.ac.za for signature
2023-06-08 - 7:36:49 AM GMT

Email viewed by tmangena@sarao.ac.za
2023-06-08 - 7:37:23 AM GMT- IP address: 66.249.93.139

Signer tmangena@sarao.ac.za entered name at signing as T.MANGENA
2023-06-08 - 7:42:46 AM GMT- IP address: 196.24.39.242

Document e-signed by T.MANGENA (tmangena@sarao.ac.za)
Signature Date: 2023-06-08 - 7:42:48 AM GMT - Time Source: server- IP address: 196.24.39.242

Document emailed to mgouws@sarao.ac.za for signature
2023-06-08 - 7:42:50 AM GMT

Email viewed by mgouws@sarao.ac.za
2023-06-08 - 7:50:49 AM GMT- IP address: 66.249.92.15

Signer mgouws@sarao.ac.za entered name at signing as Marcel Gouws
2023-06-08 - 1:44:18 PM GMT- IP address: 196.24.39.242

Document e-signed by Marcel Gouws (mgouws@sarao.ac.za)
Signature Date: 2023-06-08 - 1:44:20 PM GMT - Time Source: server- IP address: 196.24.39.242

Document emailed to sean@sarao.ac.za for signature
2023-06-08 - 1:44:21 PM GMT

Email viewed by sean@sarao.ac.za
2023-06-09 - 8:08:43 AM GMT- IP address: 196.24.39.242

Signer sean@sarao.ac.za entered name at signing as Sean Passmoor

2023-06-09 - 8:09:35 AM GMT- IP address: 196.24.39.242

Document e-signed by Sean Passmoor (sean@sarao.ac.za)

Signature Date: 2023-06-09 - 8:09:37 AM GMT - Time Source: server- IP address: 196.24.39.242

Document emailed to Sharmila Goedhart (sharmila@sarao.ac.za) for signature

2023-06-09 - 8:09:39 AM GMT

Email viewed by Sharmila Goedhart (sharmila@sarao.ac.za)

2023-06-09 - 9:19:34 AM GMT- IP address: 196.24.39.242

Document e-signed by Sharmila Goedhart (sharmila@sarao.ac.za)

Signature Date: 2023-06-09 - 9:19:48 AM GMT - Time Source: server- IP address: 196.24.39.242

Agreement completed.

2023-06-09 - 9:19:48 AM GMT